Journal of Power Sources 397 (2018) 162–169

Contents lists available at ScienceDirect

Journal of Power Sources

journal homepage: www.elsevier.com/locate/jpowsour

Surface-amorphized TiO_2 nanoparticles anchored on graphene as anode materials for lithium-ion batteries

C. Li, M. Zhao, C.N. Sun, B. Jin, C.C. Yang*, Q. Jiang**

Key Laboratory of Automobile Materials (Jilin University), Ministry of Education, School of Materials Science and Engineering, Jilin University, Changchun, 130022, China

HIGHLIGHTS

- A novel strategy has been proposed to fabricate the SA-TiO_2/RGO hybrid.
- The hybrid shows superior rate and cycling performances.
- The mechanisms behind remarkable electrochemical properties are revealed.

GRAPHICAL ABSTRACT

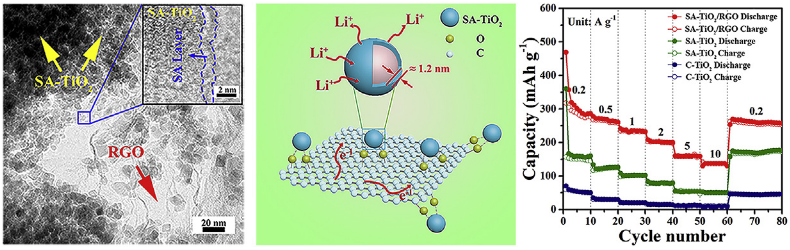

ARTICLE INFO

Keywords:
Surface amorphous structure
TiO_2 nanoparticles
Graphene
Hybrid materials
Lithium-ion batteries

ABSTRACT

One demanding challenge in the development of high-power batteries is to achieve superior rate and cycling performances. Here, we report a two-step method to fabricate a hybrid material of surface-amorphized TiO_2/reduced graphene oxide (SA- TiO_2/RGO), which exhibits superior electrochemical properties as an anode material in lithium-ion batteries, high rate property of 135.6 mAh g^{-1} at a current density of 10 A g^{-1} and cycling stability of 98 mAh g^{-1} after 2000 cycles at 5 A g^{-1}. These excellent performances originate from the unique three-dimensional integrated structure of SA-TiO_2/RGO, which provides: (i) a conductive substrate of RGO; (ii) higher conductivity of SA-TiO_2 relative to crystallized-TiO_2; (iii) ultra-small SA-TiO_2 nanoparticles; and (iv) excellent contact between SA-TiO_2 and RGO through C-O-Ti bonds.

1. Introduction

The development of high-power lithium-ion batteries (LIBs) for applications in electric vehicles, power tools, military devices, *etc.*, has attracted great attentions in recent years [1–3]. Numerous efforts have been devoted to develop electrode materials with excellent rate performance and cycling stability. Among various anode materials in LIBs, TiO_2 has drawn intensive interest thanks to its high abundance, non-toxicity, high activity, and small volume expansion upon Li^+ insertion/extraction [4,5]. However, the electrochemical performance of TiO_2 is hindered by low theoretical capacity, Li^+ mobility and electronic conductivity, as well as severe agglomeration after long-term lithiation/delithiation cycles [6].

To solve the above problems, great efforts have been implemented to construct advanced TiO_2 nanostructures and also their hybrid materials. The low Li^+ mobility has been addressed by reducing the length of diffusion channels through mesoporous [7] or nanostructured materials [8,9]; or by enhancing ion transport capacity with less-dense structural phases [10,11]. The electronic conductivity has been improved by doping TiO_2 with Nb [12]; or by coating TiO_2 with conductive mediums [13,14], such as two-dimensional reduced graphene oxide (RGO) with merits of large specific surface area, and superior electrical conductivity, structural flexibility and assembly properties. Recently, it has been demonstrated that amorphous/disordered

---

* Corresponding author.
** Corresponding author.

E-mail addresses: ccyang@jlu.edu.cn (C.C. Yang), jiangq@jlu.edu.cn (Q. Jiang).

https://doi.org/10.1016/j.jpowsour.2018.07.019
Received 19 April 2018; Received in revised form 20 June 2018; Accepted 4 July 2018
0378-7753/

materials could form percolation pathways via the opening of active diffusion channels, which not only effectively enhances mass transport within these materials, but also potentially facilitates electron and ion diffusion [15,16]. For example, Guo et al. [17] synthesized a surface-amorphized (SA) TiO_2@graphene hybrid by an ultraviolet (UV)-assisted reduction technique, which reserves the merits of surface amorphous structure, high-conductivity matrices, and well-dispersed TiO_2 nanoparticles. Thus, such a structure exhibits excellent electrochemical properties as an anode material in LIBs, a reversible capacity of 108 mAh g^{-1} after 1500 cycles at a high rate of 3.36 A g^{-1}. However, the (UV)-assisted reduction technique cannot combine TiO_2 and RGO tightly, and the electrochemical properties of the hybrid materials need further improvement.

In this work, we fabricated a hybrid material by anchoring SA-TiO_2 nanoparticles on RGO with a facial hydrothermal method. Compared with UV-assisted reduction technique, TiO_2 nanoparticles and RGO could combine tightly under the hydrothermal condition and the as-fabricated hybrid material shows superior rate performance (135.6 mAh g^{-1} at 10 A g^{-1}) and cycling stability (98 mAh g^{-1} after 2000 cycles at 5 A g^{-1}) in LIBs. The formation mechanism of SA-TiO_2 and the structure-property relationship of the hybrid material have also been elaborately discussed.

2. Experimental section

2.1. Synthesis of SA-TiO_2 and SA-TiO_2/RGO

The SA-TiO_2/RGO hybrid material was synthesized by using a two-step method. The corresponding procedure is schematically illustrated in Fig. 1. In the first step, SA-TiO_2 is obtained from hydrolysis of titanium glycolate balls, which were synthesized via the reaction of tetrabutyl titanate (TBOT) with ethylene glycol (EG) [17,18]. The combination of SA-TiO_2 and GO was achieved in the second step by using a hydrothermal method, which resulted in further crystallization of SA-TiO_2 and reduction of GO. The experimental details are given below.

4 mL tetrabutyl titanate (TBOT) and 20 mL ethylene glycol (EG) were mixed and stirred at room temperature for 12 h. Then, the above solution was added into 200 mL acetone and kept for 2 h. A white precipitate of titanium glycolate sphere was obtained by centrifugation, which was washed several times with deionized water and ethanol. After that, the white precipitate was added into the mixture of 40 mL isopropanol and 20 mL H_2O. Here, isopropanol is beneficial for controlling the hydrolysis rate and preventing the precipitation of TiO_2. Under the condition of oil bath, the above mixture was stirred for 10 h at 65 °C. The as-obtained sample was washed with deionized water and ethanol for several time, and dried in an oven at 60 °C for 12 h, obtaining SA-TiO_2. The SA-TiO_2 was annealed in air at 600 °C for 1 h to obtain crystallized-TiO_2 (C-TiO_2).

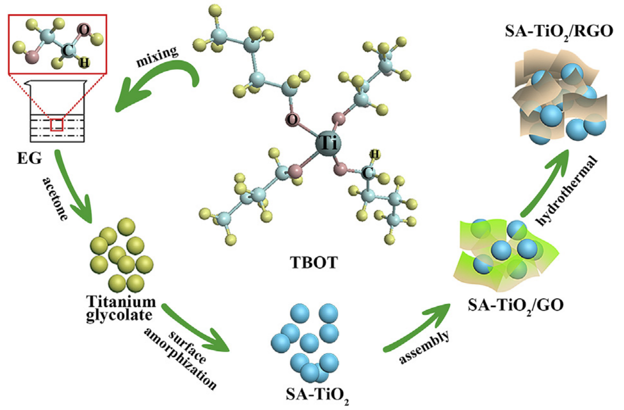

Fig. 1. Schematic illustration of the preparation procedure of SA-TiO_2/RGO.

The SA-TiO_2/RGO composite was obtained via a hydrothermal method. It should be noted that the supercritical water can exhibit strong reducing power during hydrothermal reaction. Therefore, the hydrothermal route is an efficient method for the deoxygenation reduction of GO to RGO [19–21]. In this work, graphene oxide (GO) was prepared through a modified Hummers' method. 0.2 g SA-TiO_2 was added into 80 mL GO solution (0.57 mg/mL) and thus the mass ratio of TiO_2/GO is about 4.39. After stirring for 2 h, the solution was transferred into a 100-mL Teflon-sealed autoclave and maintained at 150 °C for 5 h. The fabricated composite was recovered by centrifugation, rinsed with deionized water for several times, and fully dried in vacuum at 60 °C for 12 h, obtaining the SA-TiO_2/RGO composite.

2.2. Materials characterization

The morphology and microstructure of the samples were characterized by field-emission scanning electron microscopy (FESEM, JSM-6700 F, JEOL, 15 keV) and transmission electron microscopy (TEM, JEM-2100 F, JEOL, 200 keV). X-ray diffraction (XRD) was carried out on a D/max2500pc diffractometer using Cu-K_α radiation. X-ray photoelectron spectroscopy (XPS) analysis was performed on an ESCALAB 250 spectrometer (Thermo Fisher Scientific, UK) by using a monochromatic Al-K_α (1486.6 eV) source. Raman spectra were collected using a micro-Raman spectrometer (Renishaw) with a 532-nm laser. Thermogravimetric analysis (TGA) was performed in air at a heating rate of 10 °C min^{-1} over a temperature range of 50–800 °C using a SDT Q600 instrument.

2.3. Electrode preparation and electrochemical measurement

The working electrodes were fabricated by mixing 80% active materials, 10% conductive agent (Super P) and 10% binder polyvinylidene difluoride (PVDF) using N-methyl-2-pyrrolidone (NMP) as a solvent. The obtained slurry was pasted on Cu foil and dried in a vacuum oven at 110 °C for 12 h. To perform the electrochemical measurements for Li-ion battery, coin-type cells (CR2016) were assembled in an argon-filled glove box ($[O_2] < 1$ ppm, $[H_2O] < 1$ ppm) using as-synthesized materials as electrode active materials, lithium foil as a counter/reference electrode and Celgard 2500 membrane as the separator. The electrolyte was 1 M $LiPF_6$ dissolved in the mixture of ethylene carbonate, dimethyl carbonate and ethyl methyl carbonate with a volume ratio of 1:1:1. The galvanostatic discharge/charge curves were measured using an LAND CT2001A battery testing system in a voltage range of 1.0–3.0 V. Cyclic voltammetry (CV) measurements were conducted using an IVIUM electrochemical analyzer with a potential scan rate of 0.2 mV s^{-1} between 1.0 and 3.0 V. The electrochemical impedance spectroscopy (EIS) measurements were carried out by applying an amplitude of 10 mV over the frequency range of 100 kHz to 10 mHz.

3. Results and discussion

3.1. Characterization of hybrids

Fig. 2a compares XRD patterns of SA-TiO_2 and SA-TiO_2/RGO. The pattern of SA-TiO_2 shows typical amorphous feature with a broad peak at 25°, implying ultra-small and low-crystallized TiO_2 nanoparticles. After combining with GO under hydrothermal conditions, the fraction of the crystalline phase increases [22] as demonstrated by the XRD pattern of SA-TiO_2/RGO in the figure, where the diffraction peaks at 25.3°, 37.8°, 47.9°, 53.9°, 54.9°, 62.7° and 74.0° correspond well to the (101), (004), (200), (105), (211), (204) and (215) planes of TiO_2, which look similar to those of crystalline TiO_2 (C-TiO_2, see Fig. S1) with an anatase structure (space group: I41/amd (141), JCPDS No. 21-1272). Moreover, no obvious peak of RGO can be observed in Fig. 2a for SA-TiO_2/RGO, which indicates that the anchored TiO_2 nanoparticles prevent RGO from restacking [23]. The existence of RGO was confirmed by